Influence of the liquid layer within mixed-phase clouds on radar observations.

Lukas Pfitzenmaier[1], Yann Dufournet[1], Christine Unal[1], and Herman Russchenberg[1]

[1]*Delft Univerity of Technology, Stevinweg 1, 2628 CN, Delft, the Netherlands*
(Dated: 18 July 2014)

Lukas Pfitzenmaier

1. Introduction

Mixed-phase clouds play an important role in the earth system. They affect earth radiative balance and the climate (Comstock et al., 2007; Solomon et al., 2007) as well as the formation of precipitation (de Boer et al., 2009; Fan et al., 2011; Lamb and Verlinde, 2011). Within such mixed-phase clouds supercooled water droplets and ice particles are coexisting in the same volume and interact via microphysical processes (Shupe et al., 2008). This processes lead to growing of ice particles via Wegener-Bergeron-Findeisen process (Fan et al., 2011), riming, and/or aggregation (Lamb and Verlinde, 2011). In theory (Fan et al., 2011; Lamb and Verlinde, 2011) and in laboratory experiments (Fukuta and Takahashi, 1999) this processes are well described. Observing such processes within mixed-phase clouds is still a challenge and closely connected to the two phases and their interaction. To measure all the different properties of the hydrometeors nowadays a synergy of different instruments have to be used (de Boer et al., 2011; Shupe et al., 2008; Verlinde et al., 2013). One of the main goals is to get a better understanding of such effects of supercooled water droplets on ice crystals within mixed-phase clouds. A first step is therefore to be able to separate liquid and ice phase within such clouds. To be able to do this for any kind on mixed phase cloud type this paper show the development of a radar-based technique which allow such observations for different cloud types. This technique is also compared with standard ones using a synergy with lidar and/or microwave radiometer.

2. Liquid layer detection

Observing mixed-phase cloud processes is challenging because of two involved phases that are coexisting within this clouds. Cloud droplets have a mean droplet diameter about 10 μm (Lamb and Verlinde, 2011; Miles et al., 2000). The size range of ice crystals is much wider and spreads over 4 order of magnitude. The range is from 10 μm for simple ice plates and columns to about 1 cm for graupel and snowflakes (Lamb and Verlinde, 2011). The shape information is, however, important to characterize the different growth processes. Also the shapes of droplets and ice crystals are different and difficult to measure (Dufournet, 2010; Westbrook et al., 2010). To be able to capture all the different aspects of the involved hydrometeors nowadays a synergy of radar and lidar instruments is used (de Boer et al., 2011; Shupe et al., 2008; Verlinde et al., 2013).

2.1. Instrumental setup

Three instruments are considered in this work in order to study the detection of liquid layer within mixed-phase clouds.

2.1.1. Transportable Atmospheric RAdar - TARA

A cloud radar is using a wavelength in the mm size range that makes it able to penetrate the cloud completely. Because of the used wavelength it is sensitive to cloud droplets and ice particles and to capture the differentiation between the liquid layers and the ice crystals within the mixed-phase clouds is difficult to obtain (Rambukkange et al., 2011; Verlinde et al., 2013). A profiling precipitation radar, like the Transportable Atmospheric RAdar (TARA) from TU Delft, operates with a wavelength in the cm size range that makes it sensitive to the larger hydrometeors like precipitation droplets and the ice crystals (Dufournet, 2010). Compared to cloud radar, observing mixed-phase clouds with such a radar allows the detection of ice crystals only and not of supercooled cloud droplets (Dufournet, 2010). A direct characterization of the ice crystal properties and growth is therefore possible. Furthermore, in order to observe the shapes and size of ice crystals, the radar has to be able to make Doppler and polarimetric measurements (Fan et al., 2011; Shupe et al., 2008). Such capabilities are implemented in the TARA radar.

2.1.2. Lidar and Microwave radiometer

A lidar uses a wavelength in the nm size range it is sensitive to small hydrometeors like water droplets. It is therefore possible to retrieve the layer of supercooled liquid cloud droplets within clouds. The disadvantages of a lidar are that its signal is strongly attenuated by liquid water droplets and therefore it can not provide information during precipitation, when low water cloud are present. The microwave radiometer measured liquid water path (LWP) which represents the amount of liquid water integrated over a column of atmosphere. When supercooled water droplets are present in the cloud, the LWP is affected.

Because of the column value also precipitation and other water containing clouds contribute to this value what also limits the capability for a mixed cloud detection.

2.2. Liquid layer detection using lidar measurements

To retrieve liquid layer within mixed phase clouds a well known threshold method is used (Sassen, 1984). It uses a thresholds for lidar backscatter coefficient, that is proportional to the particle concentration, and the lidar depolarization ratio. So the retrieval defines a liquid layers by high lidar backscatter because of the with respect to ice crystals higher concentrated cloud droplets, and low depolarization ration because of the spherical shape of droplets. In Figure 2 a) the black lines show the result of such a retrieval.

2.3. Liquid layer detection using Radar bulk parameters

Due to the limitation of the instruments described in the section above, possible cloud cases with symmetric measurements are restricted to non rainy mid-level clouds without low level water clouds below. To lower the amount of limitations in this section a radar based method to detect the presence of supercooled liquid cloud droplets within mid-level clouds is proposed to be able study the growth processes of ice particles within such clouds. The method is based on changes of radar bulk parameters that are related to changes in the Doppler spectra of the radar that are based on changes in the microphysics in the radar sampling volume due to the possible presence of liquid droplets.

Identification of the cloud processes is done using scatter-plots of radar bulk parameter (see section 3). It will be shown that scatter-plots of radar bulk-parameter are a tool that makes it possible to identify microphysical processes of ice particle within the cloud system and link them also to the presence of supercooled liquid droplets. Results of the shown scatter-plots can be explained by the change of the measured radar Doppler spectrum that consequently affect the bulk parameters (see Figure 1). Using the results with additional information from lidar provide a way to detect the effect of supercooled liquid water droplets on radar bulk parameters. The different radar bulk parameters used in this work are the radar reflectivity Z

$$Z = Z_{hh} = \int_{v_{min}}^{v_{max}} |S_{hh}(v_d)|^2 \, \mathrm{d}v_d \tag{2.1}$$

which is the integral of the Doppler power spectra $|S_{hh}(v_d)|^2$ over the Doppler velocity v_d and strongly dependent on particle

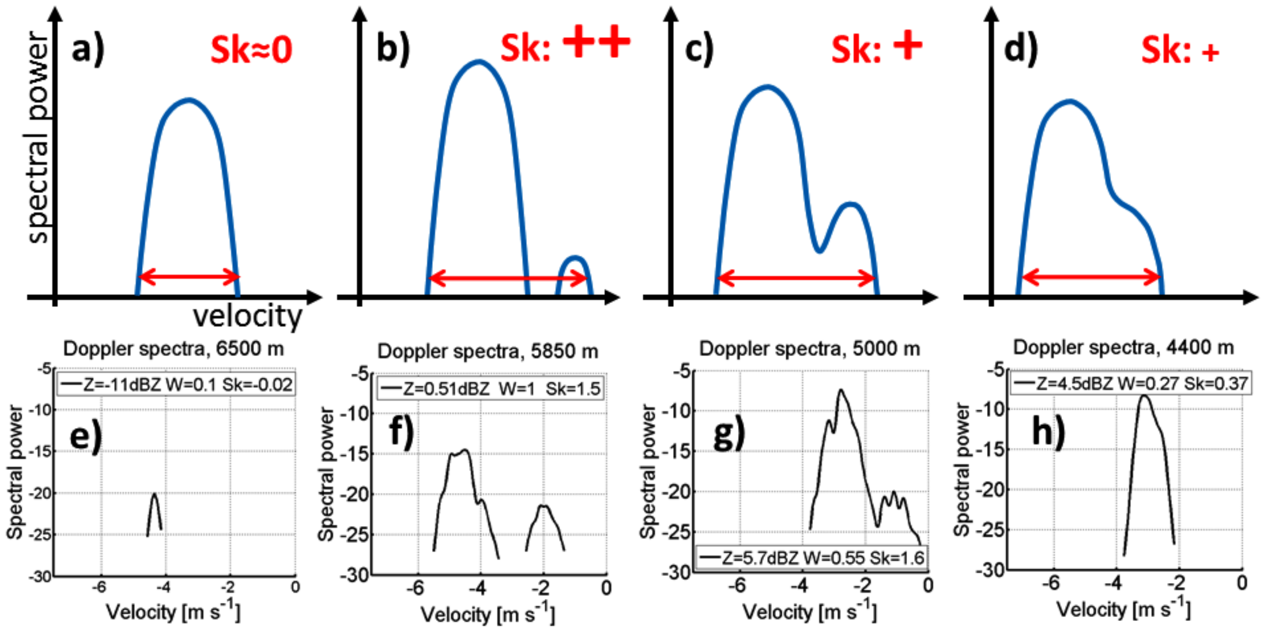

Figure 1: Shows change in radar Doppler spectra due to ice particle growth processes within-mixed phase clouds. The sketches represent different stages of particle growth and interaction with in a mixed-phase cloud. a) represents a Doppler spectra at cloud top, b), c) and d) a spectra at different stages of particle growth and interaction thwarts the cloud bottom. Blue line is the Doppler spectra, red arrows show the Doppler spectral width and the Skewness of the spectra is given on top of the sketch. High particle fall velocities are given in the negative velocity range. e) till h) represent measured Doppler spectra representing the theoretical approaches from a) to d) measured in the cloud shown Figure 2 a). e) Doppler spectra at 6650 m, $Z = -11\,\mathrm{dBZ}$, $W = 0.1\,\mathrm{m\,s^{-1}}$, $Sk = 0.02$ *, f) spectra at 5850 m* $Z = 0.5\,\mathrm{dBZ}$, $W = 1\,\mathrm{m\,s^{-1}}$, $Sk = 1.5$ *, g) at 5000 m* $Z = 5.7\,\mathrm{dBZ}$, $W = 0.55\,\mathrm{m\,s^{-1}}$, $Sk = 1.6$ *, h) Doppler spectra measured at 4400 m* $Z = 4.5\,\mathrm{dBZ}$, $W = 0.27\,\mathrm{m\,s^{-1}}$, $Sk = 0.37$

size (proportional to the sixth power of the hydrometeor size in the measured radar volume). The Doppler spectral width W is related to the second moment of the Doppler spectra,

$$W = \left(\frac{1}{Z} \int_{v_{min}}^{v_{max}} (v_d - V)^2 |S_{hh}(v_d)|^2 \, \mathrm{d}v_d \right)^{\frac{1}{2}}, \tag{2.2}$$

gives information about changes in particle size distribution or turbulence within the measured volume, where V is the mean Doppler velocity. The skewness Sk of the Doppler spectra

$$Sk = \frac{\frac{1}{Z} \int_{v_{min}}^{v_{max}} (v_d - V)^3 |S_{hh}(v_d)|^2 \, \mathrm{d}v_d}{W^3} \tag{2.3}$$

gives information about shape and asymmetry of the Doppler spectra that are related to changes in the microphysics of the particles in the measured radar volume. The last parameter that is used is the cross correlation coefficient ρ.

$$\rho = \frac{\int_{v_{min}}^{v_{max}} S_{hh}(v_d)\, S_{vv}(v_d)^* \, \mathrm{d}v_d}{\sqrt{Z_{hh} Z_{vv}}} \tag{2.4}$$

where S_{hh} and S_{vv} are the complex Doppler spectra measured in the horizontal transmitted and received polarization state or in the vertical one, respectively, and Z_{vv} the reflectivity in the $_{vv}$ state. ρ gives information about particle homogeneity within the measured volume.

In Figure 1 a) to d) shows how changes in the radar Doppler spectra affect changes in the radar bulk parameters. The blue lines represents a Doppler spectra, the red arrows indicate the Doppler width, and the expected skewness values are given in the upper corners of each sketch. At the top of the cloud, Figure 1 a), the sampling volume is dominated by small ice crystals, which lead to a mono-modal quite symmetric spectrum. The values of the bulk parameter representing such kind of spectrum leads to low reflectivity, a small Doppler width, and a skewness near zero.

Figure 1 b) shows the appearing of a second mode in the spectra, that causes a change in the ice particle microphysics at this height. The Doppler width and skewness value for this Doppler spectra are increase compared to a). The high skewness values is explained by the antisymmetry of the spectrum and the value is positive because its peak is with respect to the symmetry-axes to the negative fall velocities. The reflectivity increases too, because particles have already grown in the first mode and a second mode starts too. For the sketches a slow updraft within the clouds is assumed that leads to an appearance of the second mode in the updraft velocity range.

In Figure 1 c) the growth of the second mode got on. The reflectivity does not change much in comparison to b) the Doppler width decreases a bit, and the skewness is still high and positive. In theory it is assumed that the skewness values is smaller than in b), because the spectra goes back to a more symmetric shape but its peak is still shifted away from the symmetry-axes (compare with Figure 1 g)).

In Figure 1 d) both modes are merged and particles stop growing. Doppler width and skewness decrease even more and the reflectivity stays quit constant. This is also seen in the measured spectra in Figure 1 h) representing this stage of Doppler spectra development. So the effect of the radar bulk parameters can be drawn back to changes in the ice crystal microphysics.

2.4. Data-set

The data set of this study is based on a data-set taken during the Hydrological cycle in Mediterranean Experiment (HyMex) in the late summer and autumn 2012. TARA was located in Candillargues, France, measuring simultaneously with other sensors like microwave radiometer and the Basilicata Raman lidar (BASIL) which gave the opportunity to validate the detected growth processes within the cloud cases using this additional information.

3. Case studies

In this section the results of ice particle growth within mixed-phase clouds using a radar based method are shown. The study is based on showing mid-level cloud cases measured during HyMex (Figure 2). Case 1 (Figure 2 a)), 26^{th} September 2012, 0630-0730 UTC, represents a mixed phase cloud where supercooled liquid layer is detected from a co-located raman lidar (BASIL). The black lines are the retrieved liquid layers. It has to be pointed out that the radio sounds launched at 300 UTC and 900 UTC, both show a dry layer with a drop in relative humidity of more than 50% below at 4.5 km and 4 km, respectively. The 0°C isotherm is around 3.3 km and the temperature at cloud top height at 7 km is -21°. LWP values for that day are not available. Case 2 (Figure 2 b)), 26^{th} October 2012, 2020-2050 UTC, shows a mid-level cloud, too. For this case, no lidar data are available due to the weather conditions. However, the LWP measurements of a microwave radiometer indicates a pure ice case (below 5 g m^2 which is considered to be around the noise level of the instrument). Soundings were also not present during

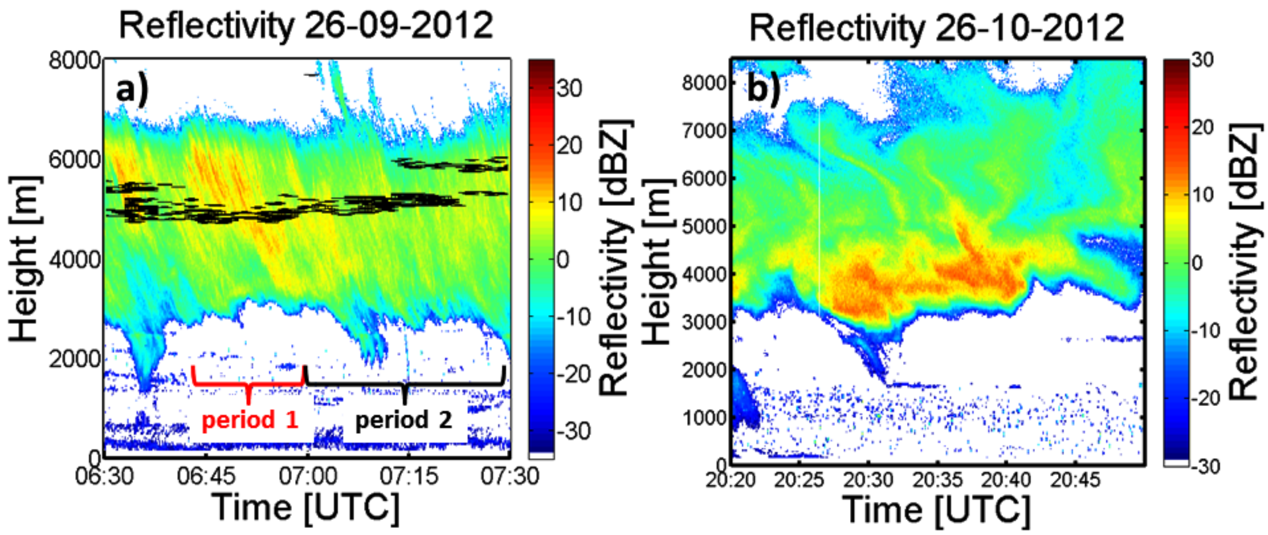

Figure 2: Plots of the two measured cloud cases. a) shows the time-height-plot of reflectivity for a mixed-phase mid-level cloud from 26th September 2012, 0630-0730 UTC. The black lines display the location of a layer of supercooled liquid cloud droplets retrieved from BASIL measurement data. The brackets show the separation of the case into, period 1 0640-0700 UTC and period 2 0700-0730 UTC. b) shows the time-height-plot of reflectivity of the second only ice containing cloud case form 26th October 2012, 2020-2050 UTC.

this case so informations about the thermodynamical states could also not be given.

3.1. Case 1 - mixed-phase cloud

Detection and analyze of the growth processes with in this cloud is done using scatter-plots of radar bulk parameter. Figure 3 shows scatter plots of Doppler width versus reflectivity for 4 different heights beginning near the cloud top (6665 m) in a) and then moving downwards through the cloud (6375 m, 5100 m, and 3999 m). a) to d) represents some scatter-plots of case 1 for period 1 and e) to h) of case 1 period 2. The color coding of the dots gives the time at which the measurement has been taken.

In the scatter-plots the growing of ice crystal can be seen by an increase of reflectivity from a) to c) for period 1. It is also seen that low reflectivity values decrease and the signal is dominated be contribution of bigger particles. In d) the particles are already influenced by the dry layer, layer top around 4 km, and stopped growing and start to evaporate. The highest values of reflectivity fall together with high values of the Doppler width, Figure 1 c). This demonstrates a change in the Doppler spectrum shape, see Figure 1 b) and c), due to a change in the ice crystal microphysics. When looking into the scatter plots for period 2 the spread of the Doppler width can already be seen at 6375 m (the red dots). Comparing this results ot the results of the retrieved liquid layer from Lidar measurements show that at this heights liquid water droplets where present. This leads to the assumption that the changes of ice crystal micrphysics come from interaction with the supercooled liquid droplets. Also g) shows similarity with c) and for both cases liquid water was retrieved by the lidar.

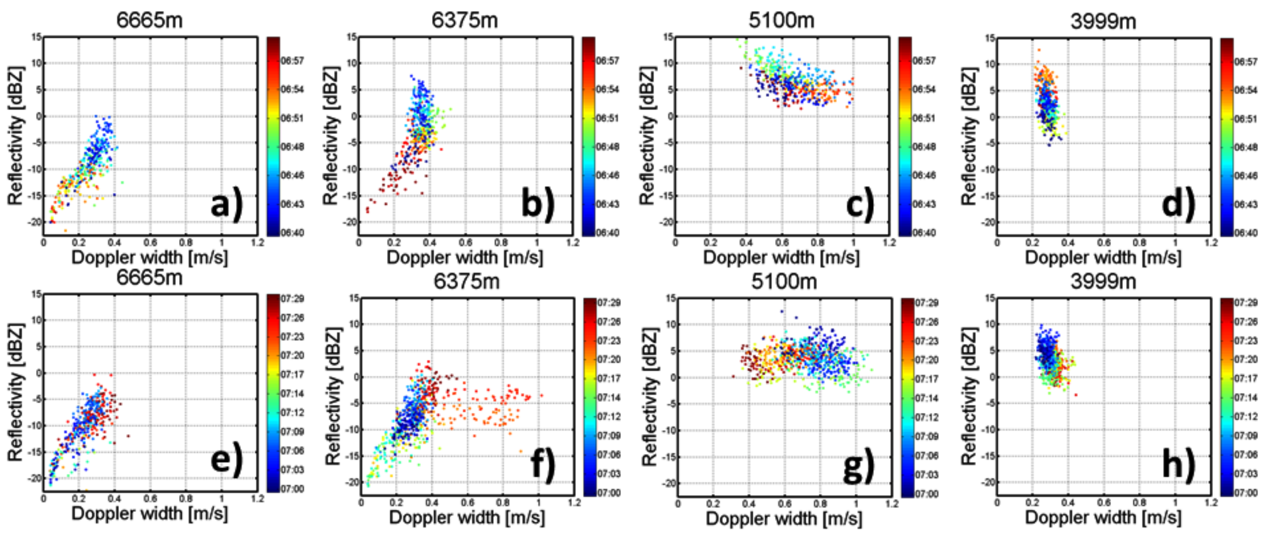

Figure 3: Case 1- mixed-phase cloud: Scatter-plots of Doppler width versus reflectivity. a) till d) show scatter-plots at 4 heights (6607 m, 5274 m, 4868 m, and 3332 m) of period 1 of the mixed-phase cloud case of Figure 2 a). e) till h) plots for the same heights for period 2. The color indicate the time of the measurement, period 1: 640 - 700 UTC, period 2: 700 - 730 UTC

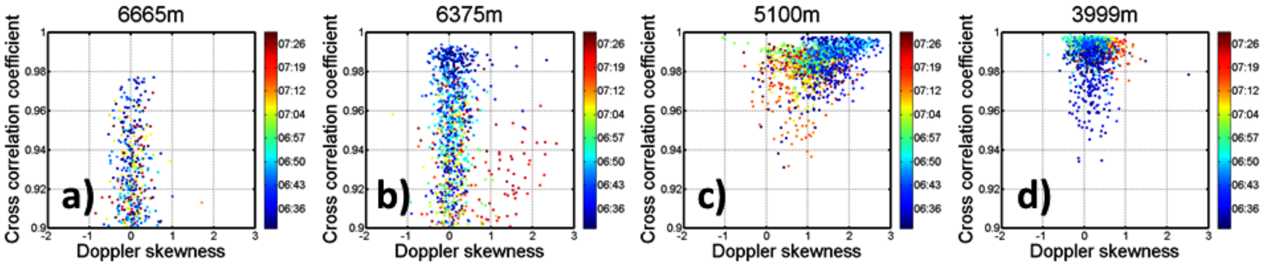

Figure 4: Case 1- mixed-phase cloud: Scatter-plots of skewness versus cross polar correlations coefficient. a) till d) show scatter-plots at 4 heights (6607, 5274 m,4868 m, and 3332 m) of the mixed-phase cloud case a) of Figure 2. The color indicate the time of the measurement, period 1: 630 - 730 UTC

The change in the microphysics can also be seen in the scatter-plots of skewness of the Doppler spectra versus the cross polar correlations coefficient in Figure 4. This plots show the whole measured cloud case 1 from 630 - 730 UTC. In this plots high skewness at 6375 m appears in the red dots, representing the last 15 minutes of the case, where also the high values in the Doppler width can be found Figure 3 f). The spread in cross correlation coefficient in a) and b) is also due to the fact that at this high the signal-to-noise-ratio is rather low and the parameter quite noisy. Figure 4 c) shows two things. First, period 1 and period 2 show different behavior in the microphysics in this height, because the center of the dots is separated. Period 1, the more blue dots, have higher skewness and cross correlation coefficient values than the more red dots indicate periode 2. High values of cross correlation coefficient are found in areas where aggregation is the dominating growth process (see later section 3.2), so it is assumed that dominant growth process between period 1 and period 2 is different. In d) the evaporation of the particles can be seen because the values spread again in cross correlation coefficient but are rather constant in skewness.

3.2. Case 2 - ice cloud

In this section a only ice crystal containing cloud is analyzed to validate assumptions from case 1 and also to show the difference in growth processes. Figure 5 shows in the top row also scatter-plots of Doppler width versus reflectivity and below the scatter-plots of skewness versus cross correlation coefficient for equal height than on the top row (7244 m, 5998 m, 4550 m, and 3709 m). In comparison to the Doppler width versus reflectivity plots in Figure 3, it can be seen, that for cloud top Figure 5 a) and Figure 3 a) and e) the plots look similar. The color coding in Figure 5 a) shows that for different time windows the growing of particles reaches different stages. The reflectivity value shows that growing of big particles in this cloud reaches its maximum at much lower height compared to case 1 (see Figure 3 c) and d)). Values in Doppler width show rather low values even for high reflectivity values. This leads to the assumption that the ice crystals grow homogeneously by aggregation. The LWP measurements for the microwave radiometer show nearly no signal so it is assumed that the cloud contains ice crystals only. Because there is no liquid involved ice crystals grow by aggregation. This is also seen in case 1 for the upper regions where it is also considered to have only ice crystals. Also the skewness versus cross correlation coefficient plots e) to h) show values near one, increases with decreasing height, which stands for a homogeneity of particles within the measured volume. This information fit quit well to the already detected slow and homogeneous growth of particles in Figure 3 a) to d). The dots of lower cross correlation in g) and h) come from already evaporating particles at this heights. This is due to that during

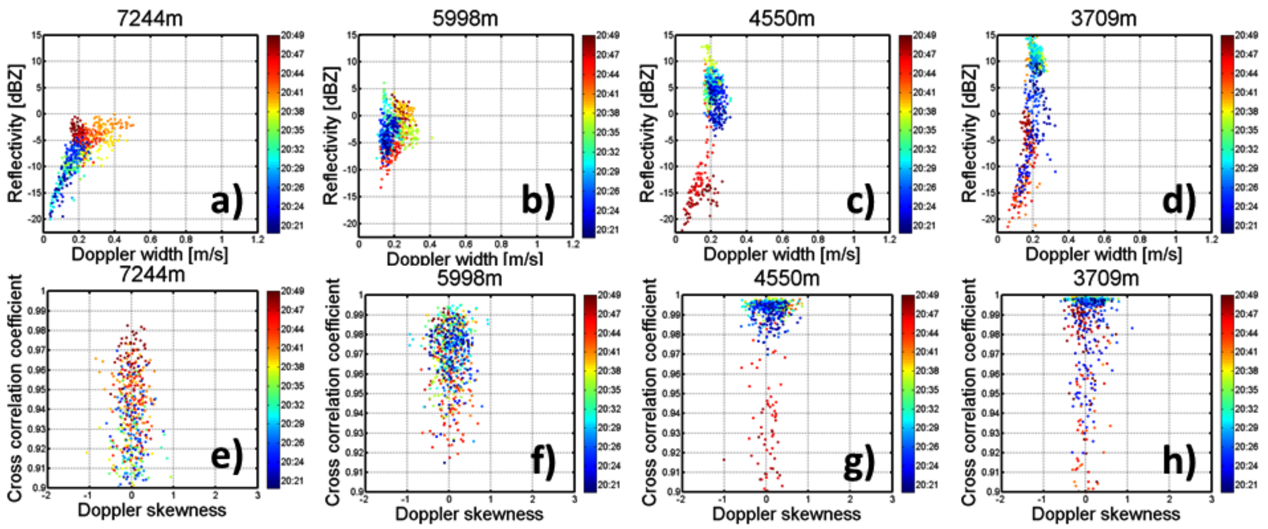

Figure 5: Case 2- ice cloud: Scatter-plots of radar bulk parameter for cloud case 2. a) till d) show scatter-plots of Doppler width versus reflectivity at 4 heights (7244 m, 5998 m, 4550 m, and 3709 m). e) till h) the scatter-plots of skewness versus cross correlation coefficient for the same 4 heights. The color of the dots indicate the time of the measurement form 2020 - 2050 UTC

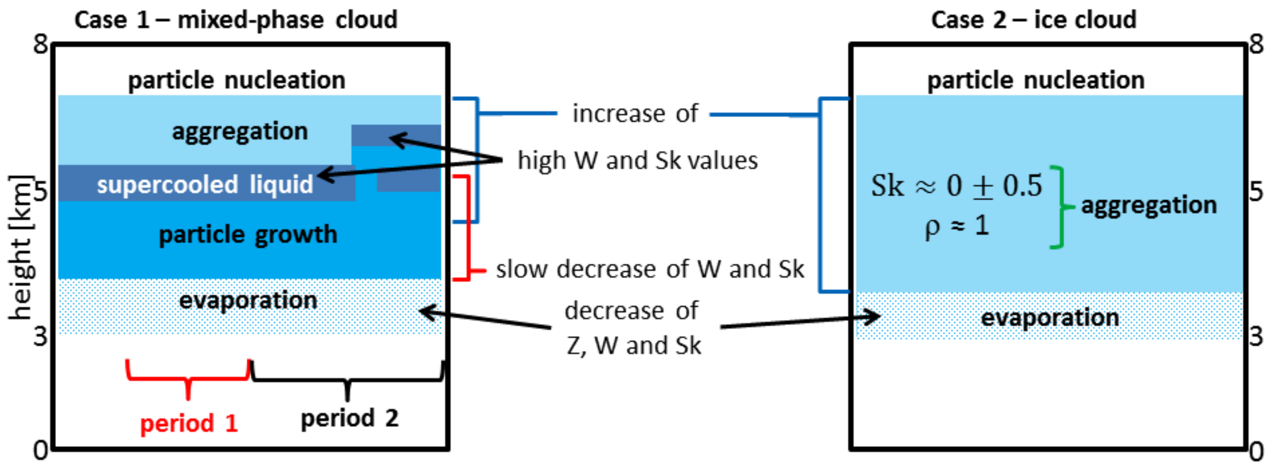

Figure 6: Scatter-plots of Doppler width versus reflectivity. a) till d) show scatter-plots at 4 heights (a)=6607 m, b)=5274 m, c)=4868 m, d)=3332 m) of period 1 of the mixed-phase cloud case a) of Figure 2, e) till h) plots at 4 heights (e)=6346 m, f)=5506 m, g)=4868 m, h)=3072 m)from period 2.

evaporation processes the homogeneity of particles within the sampling volume decreases and the cross correlation value as well. It can also be seen in c) and d) where dots in the same color show low reflectivity values.

3.3. Comparison and interpretation

Figure 6 shows in a schematic sketch the structure of the two cloud cases, including the different growth processes and thermodynamical states. The structure of the cloud is based on the interpretation of the scatter-plots in the section 3.1 and section 3.2, respectively. Similar in both cases is the nucleation of pristine ice crystals at and near cloud top and the slight growth of those particles by aggregation with decreasing height (compare Figure 3 a) and e), Figure 4 a) and e), and Figure 5 a) and e)). The structure of the scatter plots in case 2 stays till the evaporation of particles the same. Reflectivity is slightly inreasing with decreasing height, the Doppler width increases as well till it stays constant at lower heights. The value of the skewness is around 0 ± 0.5. This stands for a symmetric shape of the Doppler spectra through the whole cloud profile. So the variation within the spectra comes mainly through a wider spectrum and not through appearance of modes of new generated particles. It leads to that assumption of a homogeneous particle growth towards the cloud. Also the cross correlation coefficient shows height values that stands for particle homogeneity in the measured volume. In conclusion particle growth is happening via aggregation of ice particles in this cloud. In case 1 the structure of the scatter-plots looks different. So it is assumed that the broadening of the spectral width and the increase of the skewness in Doppler spectra is related to a change in microphysics at this heights (compare Figure 3 c) and f), Figure 4 b) and c), and section 2.3). The faster increase of reflectivity compare to the case 2 leads to the assumption that the growth processes of the ice crystals in case 1 are change compared to case 2. Faster growth and changes in the Doppler spectra lead to the assumption of interaction from ice crystals with liquid water at this height. This results are in good agreements with the supercooled water layer height(s) retrieved with the lidar technique.

4. Conclusions and Outlook

Using a radar based technique the influence of the liquid layer on the radar bulk parameters could be seen. Future steps include more case studies in order to validate the validate the radar based retrieval method. Looking into spectral data and the use of polarimetry will be done to get more information in order to characterize ice crystal microphysics and the different growth processes within the previously detected mixed-phase cloud regions.

Acknowledgement

I would like to thank Paolo Di Girolamo and Marco Cacciani from the Universita degli Studi della Basilicata, Italy, for providing me the BASIL data. I also would like to say thanks to the whole HyMex community. And finally I would like to say thank you my collages form Delft and from ITaRS (Initial training for atmospheric remote sensing) project, a Marie Curie 7 people project from the EU, for their support in this work.

References

J. M. Comstock, R. D'Entremont, D. Deslover, G. G. Mace, S. Y. Matrosov, S. A. McFarlane, P. Minnis, D. Mitchell, K. Sassen, M. D. Shupe, D. D. Turner, and Z. Wang, "An Intercomparison of Microphysical Retrieval Algorithms for Upper-Tropospheric Ice Clouds," *Bulletin of the American Meteorological Society*, vol. 88, p. 191, 2007.

G. de Boer, E. W. Eloranta, and M. D. Shupe, "Arctic Mixed-Phase Stratiform Cloud Properties from Multiple Years of Surface-Based Measurements at Two High-Latitude Locations," *Journal of Atmospheric Sciences*, vol. 66, p. 2874, 2009.

G. de Boer, W. D. Collins, S. Menon, and C. N. Long, "Using surface remote sensors to derive radiative characteristics of Mixed-Phase Clouds: an example from M-PACE," *Atmospheric Chemistry & Physics*, vol. 11, pp. 11 937–11 949, Dec. 2011.

Y. Dufournet, "Ice crystal properties retrieval ususing radar spectral polarimetric measurements wiwith ice\mixed-phase clouds," Ph.D. dissertation, Technische Universiteit Delft, 2010.

J. Fan, S. Ghan, M. Ovchinnikov, X. Liu, P. J. Rasch, and A. Korolev, "Representation of Arctic mixed-phase clouds and the Wegener-Bergeron-Findeisen process in climate models: Perspectives from a cloud-resolving study," *Journal of Geophysical Research (Atmospheres)*, vol. 116, p. 0, Sep. 2011.

N. Fukuta and T. Takahashi, "The Growth of Atmospheric Ice Crystals: A Summary of Findings in Vertical Supercooled Cloud Tunnel Studies." *Journal of Atmospheric Sciences*, vol. 56, pp. 1963–1979, Jun. 1999.

D. Lamb and J. Verlinde, *Physics and Chemistry of Clouds*, ser. 1, geïllustreerd, Ed. Cambridge University Press, 2011. [Online]. Available: http://www.cambridge.org/gb/knowledge/isbn/item5980388/?site_locale=en_GB

N. L. Miles, J. Verlinde, and E. E. Clothiaux, "Cloud droplet size distributions in low-level stratiform clouds," *Journal of Atmospheric Sciences*, vol. 57, pp. 295–311, Jan. 2000.

M. P. Rambukkange, J. Verlinde, E. W. Eloranta, C. J. Flynn, and E. E. Clothiaux, "Using Doppler Spectra to Separate Hydrometeor Populations and Analyze Ice Precipitation in Multilayered Mixed-Phase Clouds," *IEEE Geoscience and Remote Sensing Letters*, vol. 8, pp. 108–112, Jan. 2011.

K. Sassen, "Deep Orographic Cloud Structure and Composition Derived from Comprehensive Remote Sensing Measurements." *Journal of Applied Meteorology*, vol. 23, pp. 568–583, Apr. 1984.

M. D. Shupe, J. S. Daniel, G. de Boer, E. W. Eloranta, P. Kollias, C. N. Long, E. P. Luke, D. D. Turner, and J. Verlinde, "A Focus On Mixed-Phase Clouds," *Bulletin of the American Meteorological Society*, vol. 89, p. 1549, 2008.

S. Solomon, D. Qin, M. Manning, Z. Chen, M. Marquis, K. B. Averyt, M. Tignor, and H. L. Miller, Eds., *Contribution of Working Group I to the Fourth Assessment Report of the Intergovernmental Panel on Climate Change*. Cambridge University Press, Cambridge, United Kingdom and New York, NY, USA, 2007.

J. Verlinde, M. P. Rambukkange, E. E. Clothiaux, G. M. McFarquhar, and E. W. Eloranta, "Arctic multilayered, mixed-phase cloud processes revealed in millimeter-wave cloud radar Doppler spectra," *Journal of Geophysical Research (Atmospheres)*, vol. 118, p. 13199, Dec. 2013.

C. D. Westbrook, A. J. Illingworth, E. J. O'Connor, and R. J. Hogan, "Doppler lidar measurements of oriented planar ice crystals falling from supercooled and glaciated layer clouds," *Quarterly Journal of the Royal Meteorological Society*, vol. 136, pp. 260–276, Jan. 2010.